APPLIED PHYSICS LETTERS 97, 162103 (2010)

Very low surface recombination velocities on *p*- and *n*-type c-Si by ultrafast spatial atomic layer deposition of aluminum oxide

Florian Werner,[1,a)] Boris Veith,[1] Veronica Tiba,[2] Paul Poodt,[3] Fred Roozeboom,[3,4] Rolf Brendel,[1] and Jan Schmidt[1]

[1]*Institute for Solar Energy Research Hamelin (ISFH), Am Ohrberg 1, D-31860 Emmerthal, Germany*
[2]*SoLayTec, P.O. Box 6235, 5600 HE Eindhoven, The Netherlands*
[3]*TNO Science and Industry, P.O. Box 6235, 5600 HE Eindhoven, The Netherlands*
[4]*Eindhoven University of Technology, P.O. Box 513, 5600 MB Eindhoven, The Netherlands*

(Received 1 September 2010; accepted 30 September 2010; published online 20 October 2010)

Using aluminum oxide (Al_2O_3) films deposited by high-rate spatial atomic layer deposition (ALD), we achieve very low surface recombination velocities of 6.5 cm/s on *p*-type and 8.1 cm/s on *n*-type crystalline silicon wafers. Using spatially separated reaction zones instead of the conventional time-sequenced precursor dosing enables growth rates up to 70 nm/min, whereas conventional ALD limits the growth rate to <2 nm/min. The excellent passivation level is predominantly assigned to a high negative fixed charge density of $Q_f = -(4 \pm 1) \times 10^{12}$ cm^{-2} in the Al_2O_3 films. We demonstrate an excellent thermal stability of the passivation quality. © *2010 American Institute of Physics*. [doi:10.1063/1.3505311]

Amorphous aluminum oxide (Al_2O_3) films have been demonstrated to provide an excellent level of surface passivation on lightly doped *n*- and *p*-type as well as highly doped p^+-type silicon surfaces due to a high *negative* fixed charge density Q_f in the range of $-(10^{12}-10^{13})$ cm^{-2} in combination with a moderate interface state density D_{it} of $(10^{10}-10^{12})$ eV^{-1} cm^{-2} (Ref. 1 and references therein). Various deposition techniques, such as plasma-assisted and thermal atomic layer deposition (ALD),[2–5] plasma-enhanced chemical vapor deposition (PECVD),[6] and rf-sputtering,[7] have been employed. So far the best passivation quality was obtained using ALD, where both plasma-assisted and thermal ALD led to surface recombination velocities <10 cm/s.[8]

The ALD process is divided in two self-limiting half-reactions, leading to a saturation of the growth surface by exactly one monolayer of precursor molecules during each half-reaction. A controlled monolayer-by-monolayer deposition over large areas is achieved, leading to highly conformal coatings with very low pinhole densities.[3] Trimethylaluminum [TMA, $Al_2(CH_3)_6$] is commonly used as precursor gas for aluminum. Either O_2 activated by a remote plasma (plasma-assisted ALD) or water vapor at elevated temperatures (thermal ALD) is used to oxidize the TMA for growth of an amorphous Al_2O_3 layer. In a conventional ALD process, the separation of the half-reactions is implemented by alternate dosing of the process gases. Exposure times of only a few milliseconds are sufficient to ensure complete saturation of the growth surface. In between both precursor doses, however, the reactor chamber is purged by an inert gas and subsequently pumped to remove the residual process gas and reaction products. To prevent parasitic CVD processes and ensure a true ALD process, pumping times of the order of a few seconds are required, which severely limits the growth rate to approximately 2 nm/min and makes conventional ALD unsuitable for high-throughput industrial manufacturing of, e.g., silicon solar cells.

In this work, we investigate the surface passivation quality and thermal stability of aluminum oxide layers deposited by fast-rate spatially separated ALD,[9] allowing a deposition rate of 70 nm/min. In contrast to the conventional sequential separation, both half-reactions are *spatially* separated, thus eliminating the need for intermediate pumping steps. In a proof-of-principle tool the spatial separation is achieved by rotating the wafer underneath a round reactor head incorporating gas inlets for TMA and water vapor, separated by gas bearing curtains formed by a flow of pressurized nitrogen. Since both reaction zones are sealed off by nitrogen flow, any unintentional interaction of the process gases is prevented and the deposition can be performed under atmospheric conditions. In this concept, one rotation of the wafer constitutes one full ALD cycle. Figure 1 shows the thickness of an Al_2O_3 film as a function of the number of reactor head rotations. The film thickness scales linearly with the number of rotations, corroborating an ALD process at a growth per cycle of 0.12 nm/cycle. In the rotating proof-of-principle tool the Al_2O_3 film is deposited in a 3 cm wide ring-shaped track. So far, the concept has been tested up to a rotation speed of 600 rpm, corresponding to a deposition rate of 70 nm/min, constituting a significant improvement over deposition rates of <2 nm/min achieved in conventional ALD reactors. The experimental setup and deposition process have been described in more detail elsewhere.[9]

Characterization of the Al_2O_3 layers was performed on both *p*- and *n*-type 6-in. float-zone silicon (FZ-Si) wafers. The *p*-type samples were boron-doped 1.3 Ω cm shiny-etched silicon wafers of 300 μm thickness. The *n*-type samples were phosphorus-doped 1.0 Ω cm wafers, which had been etched in an aqueous potassium hydroxide (KOH) solution for 10 min to remove the saw damage, resulting in a thickness of 210 μm. To obtain symmetric test samples, each wafer was deposited on both sides by spatial ALD at a deposition rate of 14.4 nm/min. After deposition the wafers were laser-cut in 4×4 cm^2 pieces, each containing a sufficient proportion of the 3 cm wide ring-shaped track of Al_2O_3. The effective carrier lifetimes τ_{eff} were measured as a

a)Electronic mail: werner@isfh.de.

 © 2010 American Institute of Physics

IPR2025-00845
Apple-Sony EX1067 Page 1
Downloaded 08 Dec 2010 to 131.155.110.244. Redistribution subject to AIP license or copyright; see http://apl.aip.org/about/rights_and_permissions

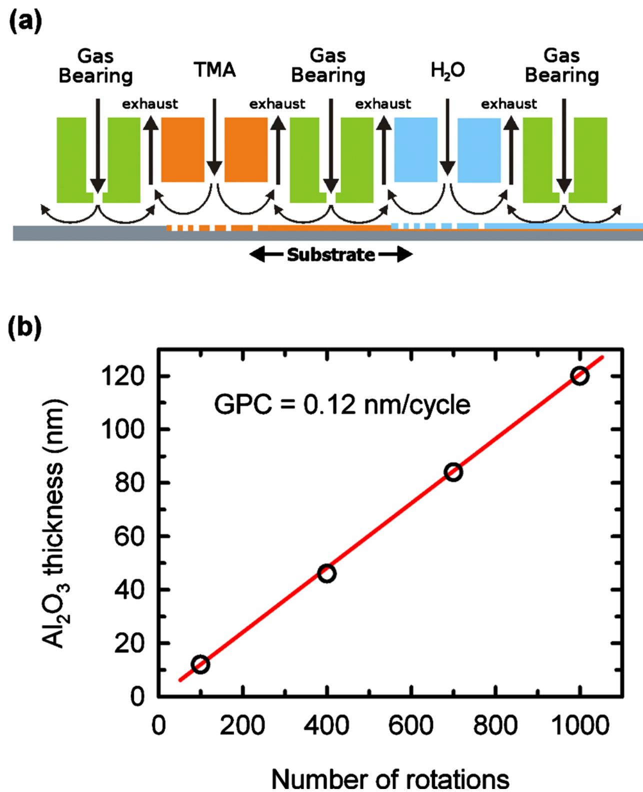

FIG. 1. (Color online) (a) Schematic drawing of the spatial ALD reactor concept, where the TMA and water half-reaction zones are separated by gas bearings. By moving the substrate underneath the reactor, the two half-reactions proceed alternatingly, forming an Al_2O_3 monolayer. (b) Al_2O_3 film thickness as a function of the number of reactor head rotations, showing a linear increase at a growth per cycle of 0.12 nm/cycle.

function of injection density Δn using a Sinton Instruments WCT-120 lifetime tester in the transient mode. The maximum effective surface recombination velocity (SRV) $S_{\text{eff.max}}$ is calculated from τ_{eff} using the following equation:[10]

$$S_{\text{eff.max}} = \frac{W}{2\tau_{\text{eff}}}, \tag{1}$$

where W is the wafer thickness. The bulk lifetime was assumed to be infinite. Accordingly, the calculated $S_{\text{eff.max}}$ value marks an upper limit to the effective SRV.

The as-deposited Al_2O_3 layers already showed a moderate level of surface passivation on p- and n-type c-Si, yielding effective lifetimes τ_{eff} ranging from 20 to 150 μs, similar to what has been observed for conventional thermal ALD.[5,8] To study the full potential for surface passivation and the thermal stability of the Al_2O_3 layers deposited in this study, we exposed the samples to a postdeposition anneal in nitrogen atmosphere, with temperatures ranging from 300 to 425 °C. Figure 2 shows the measured effective lifetime τ_{eff} at an injection level of $\Delta n = 1 \times 10^{15}$ cm^{-3} as a function of the applied thermal treatment. A "mild" anneal for 15 min at 350 °C was found to yield optimal results on the p-type as well as on the n-type silicon wafers. Figure 3 shows the injection-dependent effective lifetimes measured on p- and n-type c-Si wafers, respectively. The maximum achieved lifetimes at $\Delta n = 1 \times 10^{15}$ cm^{-3} were $\tau_{\text{eff}} = 2.3$ ms for the p-type and $\tau_{\text{eff}} = 1.3$ ms for the n-type wafers, corresponding to $S_{\text{eff.max}}$ values of 6.5 cm/s and 8.1 cm/s, respectively. The measured effective lifetimes show virtually no injection level

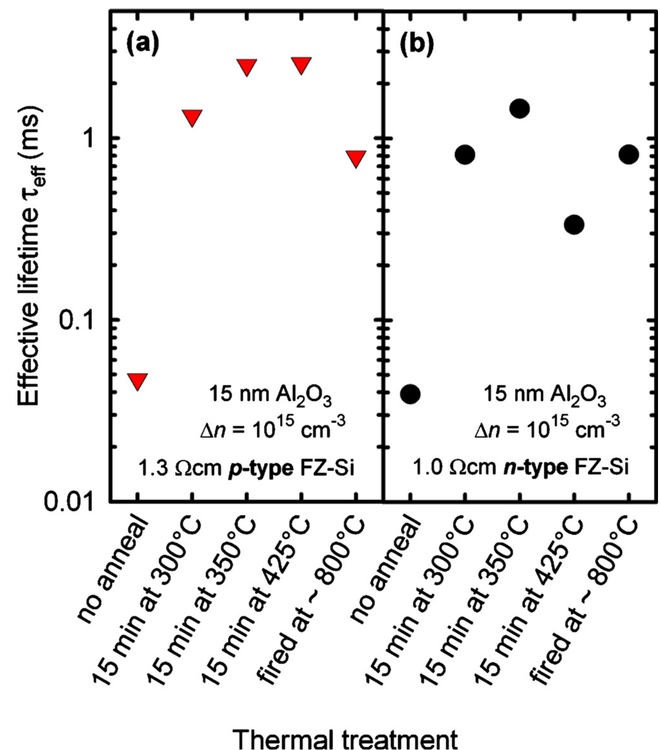

FIG. 2. (Color online) Effective lifetimes at an injection level $\Delta n = 1 \times 10^{15}$ cm^{-3} measured after different thermal treatments on p- (a) and n-type (b) FZ-Si samples for an Al_2O_3 layer thickness of 15 nm. During the firing step the wafers are kept above 600 °C for ~6 s. A "mild" anneal for 15 min at 350 °C yields optimal results.

dependence in the injection range from 10^{13} to 10^{15} cm^{-3}, which is significant for 1 sun operation of typical solar cells. As can be seen from Fig. 2, a good level of surface passivation is also achieved if the postdeposition anneal is replaced by a firing step. The Al_2O_3 layers were fired in an industrial conveyor belt furnace (Centrotherm Contact Firing Furnace DO 8.600-300-FF), as used in the production of solar cells, at a belt speed of 5.9 m/min and a set peak temperature of 920 °C, corresponding to an actual peak temperature of about 800 °C and a dwell time of ~6 s above 600 °C. The

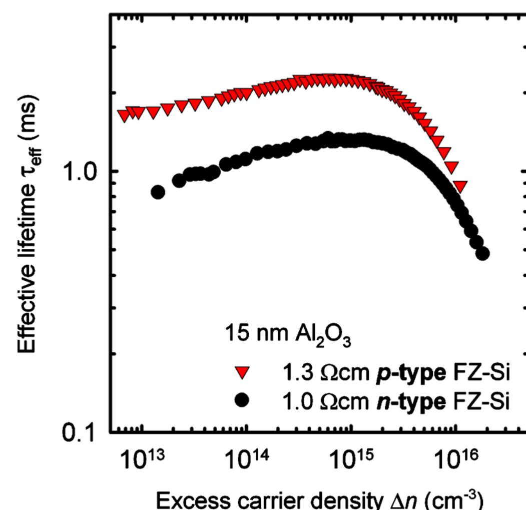

FIG. 3. (Color online) Injection-level dependent effective lifetimes τ_{eff} measured on 1.3 Ω cm p-type and 1.0 Ω cm n-type silicon samples passivated by spatial ALD. The samples were annealed for 15 min at 350 °C, the Al_2O_3 layer thickness is 15 nm.

IPR2025-00845
Apple-Sony EX1067 Page 2
Downloaded 08 Dec 2010 to 131.155.110.244. Redistribution subject to AIP license or copyright; see http://apl.aip.org/about/rights_and_permissions

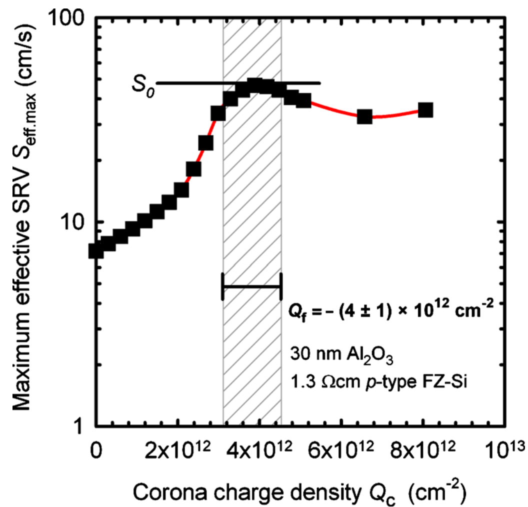

FIG. 4. (Color online) Maximum SRV $S_{eff.max}$ as a function of deposited positive Corona charge density Q_c for a 30 nm Al_2O_3 film on *p*-Si, measured at an injection density of $\Delta n = 1 \times 10^{15}$ cm^{-3}. A high negative fixed charge density $Q_f = -(4 \pm 1) \times 10^{12}$ cm^{-2} and a SRV parameter of $S_0 = 47$ cm/s are deduced. The line is a guide to the eye.

achieved lifetimes at $\Delta n = 1 \times 10^{15}$ cm^{-3} after firing were $\tau_{eff} = 790$ μs for the *p*-type and $\tau_{eff} = 815$ μs for the *n*-type wafers, corresponding to $S_{eff.max}$ values of 19.0 cm/s and 12.9 cm/s, respectively.

The very low surface recombination velocities routinely obtained on *p*- and *n*-type c-Si using laboratory-type ALD reactors are predominantly attributed to a strong field effect passivation[3] caused by a high negative fixed charge density in the Al_2O_3 film, located close to the interface. The fixed oxide charge density Q_f in our Al_2O_3 layers deposited by spatial ALD was extracted from Corona charge measurements.[11] Figure 4 shows the measured $S_{eff.max}$ as a function of the applied positive Corona charge density Q_c. A peak in the effective SRV occurs for flat band conditions, where Q_f in the Al_2O_3 layer is compensated by the deposited Q_c. We extract a high negative fixed charge density of $Q_f = -(4 \pm 1) \times 10^{12}$ cm^{-2}, which is comparable to Q_f values measured in Al_2O_3 layers deposited by conventional thermal ALD.[1] The excellent field effect passivation is accompanied by a good interface quality leading to a SRV parameter of $S_0 = 47$ cm/s at $\Delta n = 1 \times 10^{15}$ cm^{-3}, as determined from the $S_{eff.max}$ peak in Fig. 4.

In conclusion, aluminum oxide layers were deposited by spatial ALD on low-resistivity (1.3 Ω cm and 1.0 Ω cm, respectively) *p*- and *n*-type FZ-Si wafers. Effective surface recombination velocities of 6.5 cm/s were measured on *p*-type c-Si and 8.1 cm/s on *n*-type c-Si. The outstanding passivation performance was predominantly assigned to a high negative fixed charge density of $Q_f = -(4 \pm 1) \times 10^{12}$ cm^{-2}, as deduced from Corona charge experiments. The excellent firing stability and the weak injection dependence of the passivation quality makes the studied Al_2O_3 layers deposited by fast-rate spatial ALD well suited for future generations of industrial high-efficiency silicon solar cells.

Funding was provided by the state of Lower Saxony and the German Ministry for the Environment, Nature Conservation, and Nuclear Safety (BMU) under Contract No. 0325050.

[1] B. Hoex, J. J. H. Gielis, M. C. M. van de Sanden, and W. M. M. Kessels, J. Appl. Phys. **104**, 113703 (2008).
[2] G. Agostinelli, A. Delabie, P. Vitanov, Z. Alexieva, H. F. W. Dekkers, S. De Wolf, and G. Beaucarne, Sol. Energy Mater. Sol. Cells **90**, 3438 (2006).
[3] B. Hoex, J. Schmidt, P. Pohl, M. C. M. van de Sanden, and W. M. M. Kessels, J. Appl. Phys. **104**, 044903 (2008).
[4] J. Schmidt, B. Veith, and R. Brendel, Phys. Status Solidi (RRL) **3**, 287 (2009).
[5] G. Dingemans, R. Seguin, P. Engelhart, M. C. M. van de Sanden, and W. M. M. Kessels, Phys. Status Solidi (RRL) **4**, 10 (2010).
[6] P. Saint-Cast, D. Kania, M. Hofmann, J. Benick, J. Rentsch, and R. Preu, Appl. Phys. Lett. **95**, 151502 (2009).
[7] T.-T. Li and A. Cuevas, Phys. Status Solidi (RRL) **3**, 160 (2009).
[8] J. Schmidt, B. Veith, F. Werner, D. Zielke, and R. Brendel, *Proceedings of the 35th IEEE Photovoltaic Specialists Conference*, Honolulu, HI (in press).
[9] P. Poodt, A. Lankhorst, F. Roozeboom, K. Spee, D. Maas, and A. Vermeer, Adv. Mater. (Weinheim, Ger.) **22**, 3564 (2010).
[10] A. B. Sproul, J. Appl. Phys. **76**, 2851 (1994).
[11] S. Dauwe, J. Schmidt, A. Metz, and R. Hezel, *Proceedings of the 29th IEEE Photovoltaic Specialists Conference*, New Orleans, LA (IEEE, New York, 2002), p. 162.

IPR2025-00845
Apple-Sony EX1067 Page 3
Downloaded 08 Dec 2010 to 131.155.110.244. Redistribution subject to AIP license or copyright; see http://apl.aip.org/about/rights_and_permissions